Electrical tracing-assisted dual-microring label-free optical bio/chemical sensors

Junfeng Song,[1,2,*] Xianshu Luo,[1] Xiaoguang Tu,[1] Mi Kyoung Park,[1] Jack Sheng Kee,[1] Huijuan Zhang,[1] Mingbin Yu,[1] Guo-Qiang Lo,[1] and Dim-Lee Kwong[1]

[1]*Institute of Microelectronics, A*STAR (Agency for Science, Technology and Research), 11 Science Park Road, Science Park II, Singapore 117685, Singapore*

[2]*State Key Laboratory on Integrated Opto-Electronics, College of Electronic Science and Engineering, Jilin University, Changchun 130012, China*

songjf@ime.a-star.edu.sg

Abstract: We propose and demonstrate a novel electrical tracing-assisted dual-microring resonator-based optical sensor system in silicon-on-insulator substrate. The system comprises one microring resonator-based sensing element and another microring resonator-based tracing element integrated with electrical controller. The resonance wavelength shift of sensing microring induced by the refractive index change is traced and determined by direct voltage supply of the electrical tunable tracing microring. Such optical sensing system eliminates the traditional wavelength-scanning method thus provide a cost effective sensing scheme. Proof-of-principle demonstration by testing polyelectrolyte multilayer shows the sensitivity of ~4.0 mW/ng·mm^{-2} and the detection limit of ~5.35 pg/mm^2.

OCIS codes: (130.6010) Sensors; (280.1415) Biological sensing and sensors; (280.4788) Optical sensing and sensors; (130.3120) Integrated optics devices; (130.7408) Wavelength filtering devices.

References and links

1. F. S. Ligler and C. A. R. Taitt, *Optical Biosensors: Present and Future* (Gulf Professional Publishing, 2002).
2. R. Narayanaswamy and O. S. Wolfbeis, *Optical Sensors: Industrial, Environmental and Diagnostic Applications*, 1st ed. (Springer, 2004).
3. X. Fan, I. M. White, S. I. Shopova, H. Zhu, J. D. Suter, and Y. Sun, "Sensitive optical biosensors for unlabeled targets: a review," Anal. Chim. Acta **620**(1-2), 8–26 (2008).
4. M. E. Stewart, C. R. Anderton, L. B. Thompson, J. Maria, S. K. Gray, J. A. Rogers, and R. G. Nuzzo, "Nanostructured plasmonic sensors," Chem. Rev. **108**(2), 494–521 (2008).
5. J. Homola, *Surface Plasmon Resonance Based Sensors* (Springer, 2006).
6. B. J. Luff, J. S. Wilkinson, J. Piehler, U. Hollenbach, J. Ingenhoff, and N. Fabricius, "Integrated Optical Mach–Zehnder Biosensor," J. Lightwave Technol. **16**(4), 583–592 (1998).
7. A. Brandenburg, "Differential refractometry by an integrated-optical Young interferometer," Sens. Actuator B-Chem. **39**(1-3), 266–271 (1997).
8. M. E. Bosch, A. J. Ruiz Sánchez, F. S. Rojas, and C. B. Ojeda, "Recent Development in Optical Fiber Biosensors," Sensors (Basel Switzerland) **7**(6), 797–859 (2007).
9. D. J. Monk and D. R. Walt, "Optical fiber-based biosensors," Anal. Bioanal. Chem. **379**(7-8), 931–945 (2004).
10. B. Cunningham, P. Li, B. Lin, and J. Pepper, "Colorimetric resonant reflection as a direct biochemical assay technique," Sens. Actuator B-Chem. **81**(2-3), 316–328 (2002).
11. S. Mandal, J. M. Goddard, and D. Erickson, "A multiplexed optofluidic biomolecular sensor for low mass detection," Lab Chip **9**(20), 2924–2932 (2009).
12. M. R. Lee and P. M. Fauchet, "Two-dimensional silicon photonic crystal based biosensing platform for protein detection," Opt. Express **15**(8), 4530–4535 (2007).
13. R. W. Boyd and J. E. Heebner, "Sensitive disk resonator photonic biosensor," Appl. Opt. **40**(31), 5742–5747 (2001).
14. F. Vollmer and S. Arnold, "Whispering-gallery-mode biosensing: label-free detection down to single molecules," Nat. Methods **5**(7), 591–596 (2008).
15. D.-X. Xu, M. Vachon, A. Densmore, R. Ma, A. Delâge, S. Janz, J. Lapointe, Y. Li, G. Lopinski, D. Zhang, Q. Y. Liu, P. Cheben, and J. H. Schmid, "Label-free biosensor array based on silicon-on-insulator ring resonators addressed using a WDM approach," Opt. Lett. **35**(16), 2771–2773 (2010).

#156193 - $15.00 USD Received 10 Oct 2011; revised 9 Nov 2011; accepted 10 Nov 2011; published 6 Feb 2012

16. K. De Vos, I. Bartolozzi, E. Schacht, P. Bienstman, and R. Baets, "Silicon-on-insulator microring resonator for sensitive and label-free biosensing," Opt. Express **15**(12), 7610–7615 (2007).
17. M. Iqbal, M. A. Gleeson, B. Spaugh, F. Tybor, W. G. Gunn, M. Hochberg, T. Baehr-Jones, R. C. Bailey, and L. C. Gunn, "Label-free biosensor arrays based on silicon ring resonators and high-speed optical scanning instrumentation," IEEE J. Sel. Top. Quantum Electron. **16**(3), 654–661 (2010).
18. T. Claes, J. G. Molera, K. De Vos, E. Schacht, R. Baets, and P. Bienstman, "Label-free biosensing with a slot-waveguide-based ring resonator in silicon on insulator," IEEE Photonics J. **1**(3), 197–204 (2009).
19. C.-Y. Chao, W. Fung, and L. J. Guo, "Polymer microring resonators for biochemical sensing applications," IEEE J. Sel. Top. Quantum Electron. **12**(1), 134–142 (2006).
20. J. Song, Q. Fang, X. Luo, H. Cai, T.-Y. Liow, M. B. Yu, G. Q. Lo, and D.-L. Kwong, "Thermo-optical tunable planar ridge microdisk resonator in silicon-on-insulator," Opt. Express **19**(12), 11220–11227 (2011).
21. J. Song, Q. Fang, S. H. Tao, T.-Y. Liow, M. B. Yu, G. Q. Lo, and D.-L. Kwong, "Fast and low power Michelson interferometer thermo-optical switch on SOI," Opt. Express **16**(20), 15304–15311 (2008).
22. G. Decher, "Fuzzy Nanoassemblies: Toward Layered Polymeric Multicomposites," Science **277**(5330), 1232–1237 (1997).
23. C. A. Barrios, M. J. Bañuls, V. González-Pedro, K. B. Gylfason, B. Sánchez, A. Griol, A. Maquieira, H. Sohlström, M. Holgado, and R. Casquel, "Label-free optical biosensing with slot-waveguides," Opt. Lett. **33**(7), 708–710 (2008).
24. Q. Fang, J. F. Song, T.-Y. Liow, H. Cai, M. B. Yu, G. Q. Lo, and D.-L. Kwong, "Ultralow Power Silicon Photonics Thermo-Optic Switch With Suspended Phase Arms," IEEE Photon. Technol. Lett. **23**(8), 525–527 (2011).

1. Introduction

Label-free optical biosensors are essential in the application of medical diagnosis, healthcare and environmental monitoring [1–3]. Various kinds of the optical biosensors are proposed and demonstrated, including surface plasmonic resonance-based devices [4,5], optical interferometers [6,7], optical fiber devices [8,9], grating and photonic crystal structures [10–12], and microresonator (microdisk, microsphere, microring) biosensors [13–16]. Among all the approaches, silicon-on-insulator (SOI) microresonator-based biosensors have been attracting much of research interests due to the high sensitivity to refractive index change, the compact footprint for large-scale integration, the compatibility with CMOS technology, and potential large-scale-integration with micro-fluidics. Single microring resonator-based biosensors in SOI have been demonstrated using either conventional microrings or slot-waveguide microring, with detection limit ranges from 10^{-4}~10^{-7} RIU [15–19]. In general, there are two basic methods for optical sensing, including wavelength scanning method [15–18] and intensity scanning method [19]. However, as the sensitivity of the intensity scanning method depends on the probe wavelength and the sensitivity of the photodetectors in order to ensure high signal-to-noise ratio to maximize the intensity change, most of the demonstrated microresonator-based sensors adopt the wavelength-scanning method for measuring the sharp resonance wavelength shift. In the other hand, the wavelength-scanning method requires expensive high-resolution wavelength tunable lasers, and thus the detection limit is ultimately limited by the laser resolution. Therefore, the high-resolution wavelength-scanning method might not be suitable for cost-effective point-of-care applications.

In this paper, we propose a novel electrical tracing-assisted bio/chemical sensing system, which comprises one microring resonator as the sensing element and another tunable microring resonator as tracing element. The resonance shift of the sensing microring can be traced and extracted from the voltage supply to the tracing microring. We demonstrate the proposed sensing system in silicon-on-insulator (SOI) by using thermally tunable microring resonators. Proof-of-principle demonstration by testing polyelectrolyte multilayer shows the sensitivity of 4.0 mW/ng·mm^{-2} and the detection limit of ~5.35 pg/mm^2.

2. Operating principle

Figure 1(a) shows the schematic of the sensing system, which comprises two serially cascaded add-drop microring resonators with similar dimensions. The first microring senses the effective refractive index change, termed as the *sensing element*, while the second microring traces the resonance wavelength shift of the sensing element by either thermo-optic

#156193 - $15.00 USD Received 10 Oct 2011; revised 9 Nov 2011; accepted 10 Nov 2011; published 6 Feb 2012

(TO) or electro-optic (EO) effect, termed as *tracing element*. A broad-band light that inputs from input-port goes through the sensing microring, and feeds into the tracing microring from the drop-port of the sensing microring. If we control the wavelength range of the broadband light source to be less than the free-spectral range (FSR), there is only one resonance for both microrings. Then, the output intensity from output-port reaches the maximum only when both resonances align with each other, according to the filter-cascading effect. Otherwise, the output power will be at the minimum. Figures 1(b) and 1(c) show the working principle of the proposed sensing system. The upper rows show the separate resonance locations of both microrings, while the lower rows show the output intensity distribution. By scanning the power supplying to the tracing microring while monitoring the output intensity, the resonance shift of the sensing microring due to the refractive index change, $\Delta\lambda_s(\Delta n)$ can related to the resonance wavelength shift of the tracing microring due to the power supply, $\Delta\lambda_t(W_2)$ - $\Delta\lambda_t(W_1)$. Thus, the effective refractive index change can be extracted from the power change.

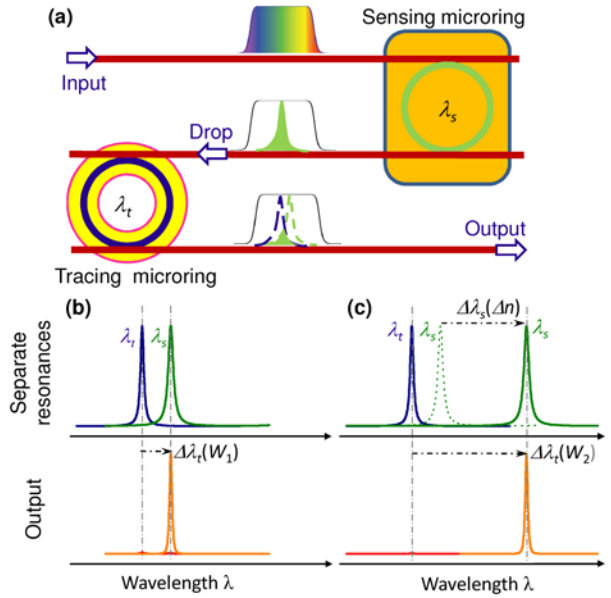

Fig. 1. (a) Schematic of the proposed electrical tracing-assisted dual-microring resonator-based optical sensing system, which adopts two serial cascaded add-drop microring resonators. (b), (c) Working principle of the sensor system. (b) Before refractive index change. The tracing microring requires electrical power W_1 in order to trace and align the resonances with that of the sensing microring. (c) After refractive index change. The resonance shift of the sensing microring due to the refractive index change Δn is $\Delta\lambda_s$, which requires W_2 electrical power for the tracing microring to trace and align with the shifted resonance. The effective index change Δn can be extracted from the electrical power change of $W_2 - W_1$.

If we choose voltage mode of the power supplier in a thermo-optically tunable microring, the sensing detection limit depends on the resolution of the voltage supplier. For the tracing microring, the resonance wavelength according to the supplied voltage can be expressed as

$$\lambda_t = AW + C = AV^2 / R + C \tag{1}$$

where A is the thermo-optic coefficient, R is the heater resistance, and C is a constant value. Thus, the resonance wavelength shift is:

$$\Delta\lambda_t = A\Delta W = 2AV\Delta V / R \tag{2}$$

#156193 - $15.00 USD Received 10 Oct 2011; revised 9 Nov 2011; accepted 10 Nov 2011; published 6 Feb 2012

It clearly shows that the resonance shift depends on the voltage resolution ΔV. As the refractive index change Δn can be extracted from the resonance shift of the tracing microring $\Delta\lambda_t$, the detection limit of the Δn depends on the electrical power resolution.

3. Device design and fabrication

We perform the proof-of-principle demonstration of our proposed sensing system by using dual-microring cascading system in silicon-on-insulator platform. Figure 2(a) shows the layout design of the proposed dual-microring resonator-based optical sensor system. Here we design the sensing system with 3 input ports and 3 output ports in order to separately measure the optical properties of both microrings. From transmission 1-1' and 3-3′, we can separately measure the drop-port optical responses of the tracing microring and sensing microring. From 2 to 2', we can demonstrate the principle of the proposed sensing system use both microrings.

In general, the small cross-sectional waveguides are better for high sensitivity sensing as more optical field extends outside of the waveguide to interact with the sensing object. However, the small waveguide tends to with higher transmission loss, thus limiting the detectable intensity and reduce the detection limit. In this demonstration, we chose the waveguide with dimension of 400 nm × 220 nm. The coupling length and coupling gaps between side-coupled waveguide and microrings are 20 μm and 400 nm, respectively. Both microrings are designed identically with 10 μm radius. We adopt thermo-optic effect for the resonance tunability of the tracing microring for the simply fabrication process. According to Eq. (2), the large electrical resistance is favorable for small detection limit. Thus, we choose a narrow width TiN strip with folded structure as the thermal heater. Both width and gap of the heater strip are 1.5 μm. We mention that in order to minimize the effect of the microfluidic flow, the thermally tunable microring separate ~4 mm from the sensing microring, which is practically covered with microfluidics cell.

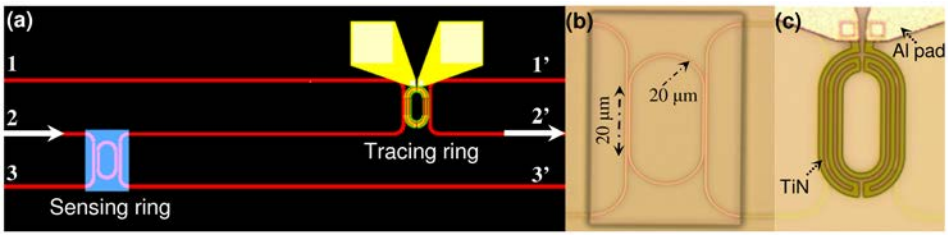

Fig. 2. (a) Layout design of the dual-microring based sensing system. Optical microscopes of the fabricated (b) sensing microring, and (c) tracing ring integrated with thermal heater.

The fabrication process is similar with the thermo-optic switch [20,21]. We started the fabrication on a commercially available 200 mm SOI wafer with 220 nm-thick top silicon layer and 2 μm-thick buried oxides (BOX) layer. Firstly, the microring structures is patterned by 248 nm deep UV lithography and etched to BOX by reactive ion etching (RIE) process. Two spots size converter (SSC) are fabricated at input- and output-coupling facets in order to reduce coupling losses between the lensed fiber and the waveguide. Then ~1.5 μm high-density plasma (HDP) oxide is deposited, followed by 150 nm Titanium nitride (TiN) deposition for the thermal heater. A 30 nm-thick silicon nitride is deposited for TiN etching protection. After the formation of contact holes, ~750 nm thick aluminum is deposited, followed by metal pad etching. Finally, the sensing window is opened for the sensing microring by RIE dry etch. Figures 2(b) and 2(c) show the optical microscope of the fabricated sensing microring and the tracing microring.

#156193 - $15.00 USD Received 10 Oct 2011; revised 9 Nov 2011; accepted 10 Nov 2011; published 6 Feb 2012

4. Device characterizations and results discussion

4.1 Spectra response of the tracing microring

For understanding of the thermal tuning capability, we first characterize the spectra responses of the tracing microring by measuring 1-1' transmission. Figure 3(a) shows the measured transmission spectra of the tracing microring upon voltage change from 0 V to 8 V with 1 V step. The transmission is normalized to a reference waveguide transmission. The free-spectral range (FSR) is ~5.66 nm and the Q factor is ~10,000. As the increases of the supplied voltage, the resonance shows red-shift. Based on the current-voltage measurement, we extract the electrical resistance of ~1.420 kΩ. Thus, the power consumption according to every voltage supplies can be calculated. Figure 3(b) shows the measured resonance positions as functions of the supplied electrical powers. We linearly fit such wavelength change and obtain the thermal tuning efficiency to be ~0.1 nm/mW.

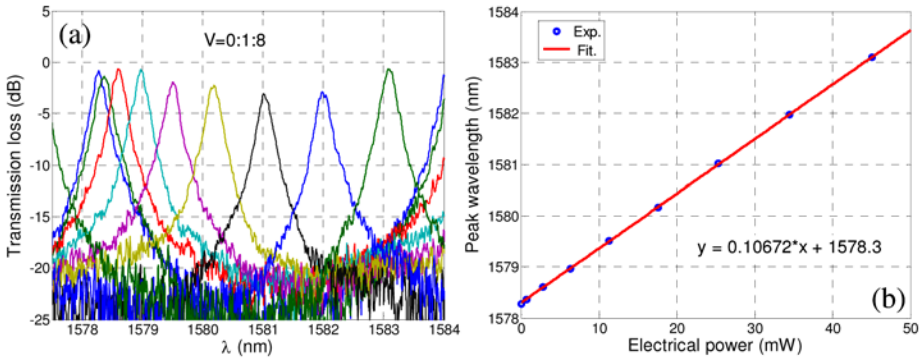

Fig. 3. (a) Measured transmission spectra of the tracing ring upon different DC voltages. (b) Resonance wavelength positions as functions of the supplied electrical powers. Linear fitting shows the thermal tuning efficiency of ~0.1 nm/mW.

4.2 Electrical tracing-assisted optical sensing measurement

Here we show the proof-of-principle demonstration of the proposed electrical tracing-assisted optical sensing measurement. We determine the refractive index change of the sensing microring from the supplied electrical power to the tracing microring by testing the formation of polyelectrolyte multilayer. Polyelectrolyte multilayer can be easily prepared by the layer-by-layer deposition of oppositely charged polyelectrolytes. Ordered multilayer assemblies are formed on a solid substrate by sequentially dipping a substrate into an aqueous solution containing polyelectrolytes of opposite charge and allowing the polyelectrolytes to spontaneously adsorb. This method has shown to produce polymer films with high uniformity (surface roughness < 0.1 nm) and a well-defined controllable thickness [22]. The device is firstly treated with oxygen plasma and immersed in a solution of 2% 3-aminopropyltriethoxysilane (APTES) in a mixture of ethanol/H_2O (95%/5%, v/v) for 2 hours, followed by thoroughly rinsing with ethanol and DI water, and then dried under a nitrogen stream. APTES molecules bind to the hydroxyl-terminated SiO_2 surfaces of the microring device, resulting in an amine-functionalized surface, which forms positive-charged surface in neutral pH. Polyelectrolyte multilayer film is built by alternately immersing the device in aqueous solutions of poly(sodium-4-styrenesulfonate) (PSS, 1 mg/mL in 50 mM NaCl) and poly(allylamine hydrochloride) (PAH, 1 mg/mL in 50 mM NaCl) for 15 min each. After each PSS/PAH deposition, the device is rinsed three times in DI water and nitrogen drying. By repeating PSS and PAH deposition, we can attain different periods of layer-by-layer PSS/PAH covering on the sensing microring waveguide surface. We measure the sensitivity of $(PSS/PAH)_N$ with N starting from 5.

#156193 - $15.00 USD Received 10 Oct 2011; revised 9 Nov 2011; accepted 10 Nov 2011; published 6 Feb 2012

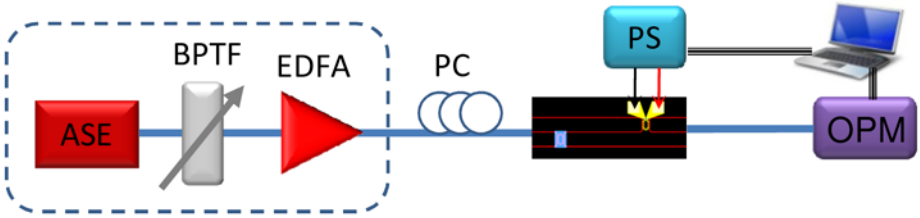

Fig. 4. Testing setup of tracing-, sensing-ring biosensor. BPTF: Band pass tunable filter. PC: Polarization controller. PS: power supply. OPM: Optical power meter.

Figure 4 shows the schematic of the characterization setup. The amplified spontaneous emission (ASE EXFO FLS-2300B) and band-pass tunable filter are used as a wide-band light source. An EDFA is used to boost optical power before entering into the device under test. The polarization controller is used to control the light to be TE polarization. The light is coupled from the polarization-maintain single mode lensed fiber to the spot size converter. The output light is also coupled from a spot size converter to another lensed single mode fiber and detected by an optical power meter. Both the power meter (Newport 2832C) and the power supplier (Agilent E3640A) are remotely controlled simultaneously.

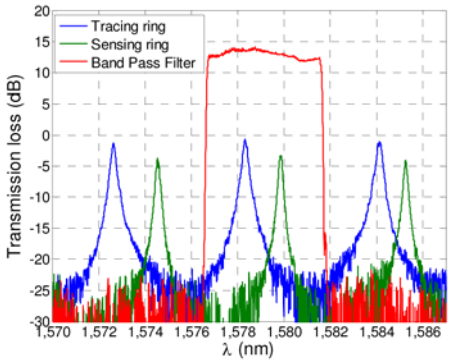

Fig. 5. Measured transmission spectra for the tracing ring (1-1', blue line), the sensing ring (3-3′, greed line) and the tunable filter (red line).

We first measure the optical transmission spectrum of the sensing microring in order to determine the wavelength range of the input light. Figure 5 shows the measured sensing microring spectrum (in green), comparing to that of the tracing microring (in blue). For the sensing microring, the FSR is ~5.2 nm and the Q-factor is ~9000. Furthermore, the drop-port intensity is relatively low for the sensing microring. We mention that although we design identically the sensing microring and the tracing microring, the different cladding makes the differences of the FSRs, the Q-factors, and the drop-port intensities due to stronger light confinement in the sensing microring from the larger refractive index difference. The red line in Fig. 5 shows the input light wavelength window from the ASE and the band-pass tunable filter for the testing. The wavelength range of the output light is controlled to be ~5 nm, which is narrower than one FSR of the sensing microring. The limited wavelength range includes only one resonance for both sensing and tracing microrings, thus promising the output power only with one peak during the electrical power scanning.

With fixed broadband input light, we measure the 2-2' transmissions while scanning the power supplies to the tracing microring. Figure 6(a) shows the measured optical responses of the sensing system as functions of the scanning electrical powers with PSS/PAH periods ranging from 5 to 10. The electrical powers are calculated by using $W = V^2/R$. The effective refractive index of the sensing microring increases as the increase of the PSS/PAH period,

#156193 - $15.00 USD Received 10 Oct 2011; revised 9 Nov 2011; accepted 10 Nov 2011; published 6 Feb 2012

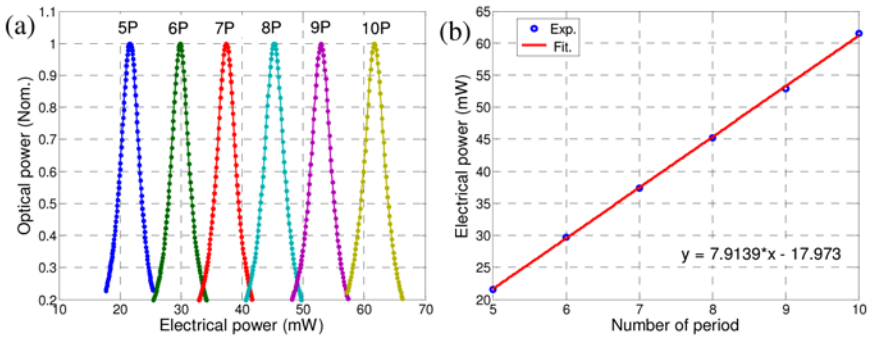

Fig. 6. (a) Optical response for different polymer periods. (b) Linear fitting for electrical power according to maximum optical response.

corresponding to the red-shifted resonances. Thus, the required electrical powers for the tracing microring to trace and align with such resonances increase. Figure 6(b) shows the electrical powers as function of the periods of the PSS/PAH layers. Linear fitting shows a relation of 7.9 mW/period, suggesting equally increased refractive index for every PSS/PAH layer. For each period of the PSS/PAH layer deposited from solution with ionic strength of 50 mM NaCl, the surface density is ~2.0 ng/mm^2. Thus, the sensing sensitivity is S ~4.0 mW/ng·mm^{-2}.

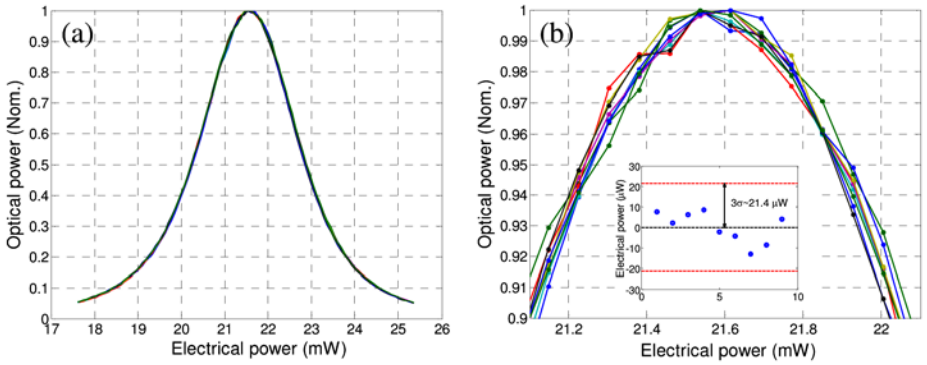

Fig. 7. (a) Normalized optical power vs. electrical voltage. (b) Zoom-in views of the optical power in range of 0.9~1. Inset: the distribution of fitted electrical powers at the peak powers.

As shown in Eq. (2), the detection limit relates to the electrical power resolution, which can be determined by measuring the standard deviation σ of the supplied electrical power. Figure 7(a) shows as an example the transmission intensities as function of the electrical power with 5 periods of PSS/PAH layer. We repeat the measurement for 9 times with the voltage step of 10 mV. The zoom-in views of the intensity distributions around peak intensity are shown in Fig. 7(b). The peak positions of every measurement can be extracted by mathematic fitting the optical response. Here we show that the optical responses according to the electrical power supplies are still Lorentzian function.

As the intensity readout from the optical power meter is the integration of the optical power in the whole spectrum range, the optical power response to the supplied electrical power can be determined by the following equation:

$$\int_0^{+\infty} F_s(\lambda) F_t(\lambda) d\lambda = \int_0^{+\infty} \frac{1}{1+4(\lambda-\lambda_s)^2/\delta_s^2} \frac{1}{1+4(\lambda-\lambda_t)^2/\delta_t^2} d\lambda = \frac{\pi\delta_s\delta_t}{2(\delta_s+\delta_t)} \frac{1}{1+4(\Delta W)^2/(\delta_s/A+\delta_t/A)^2} \quad (3)$$

#156193 - $15.00 USD Received 10 Oct 2011; revised 9 Nov 2011; accepted 10 Nov 2011; published 6 Feb 2012

where $F_s(\lambda)/F_t(\lambda)$, λ_s/λ_t, δ_s/δ_t, are the Lorentzian responses, the resonance wavelegnths and the full-width at half-maximum (FWHMs) of the sensing and tracing microrings. ΔW is the electrical power changes and A is the power supplying coefficient. From Eq. (3), the output optical power is still a Lorentzian response to the supplied electrical power, while the FWHM relates to the FWHMs of the sensing and tracing microrings.

By fitting all the 9 output power response to the supplied electrical powers using Lorentzian lineshapes, we obtain the electrical powers corresponding to the optical peak intensity, which are shown as the inset in Fig. 7(b). The extracted 3σ is δW ~21.4 μW. Thus, the detection limit can be calculated as: DL = $\delta W/S$ = 5.35 pg/mm^2.

4.3 Wavelength-scanning measurements

In order to confirm the measurements by electrical tracing technique, here we show the measurements by using wavelength-scanning method with 3-3′ transmissions. Such optical transmission spectra are measured together with the electrical measurements. Figure 8(a) shows the measured transmission spectra of the sensing microring with PSS/PAH layer changing from 5 to 10. The increase of the PSS/PAH layer increase the cladding refractive index, thus red-shift the resonance wavelength. Figure 8(b) shows the resonance wavelength positions as the function of the PSS/PAH layer periods. The linear fitting shows a sensing sensitivity of ~0.786 nm/period. Considering the thermal efficiency for the tracing microring is ~0.107 nm/mW, it corresponds to ~7.35 mW/period. This is consistent to the demonstrated ~7.9 mW/period by the electrical tracing technique, which confirmed the validation of the proposed electrical tracing-assisted sensing system.

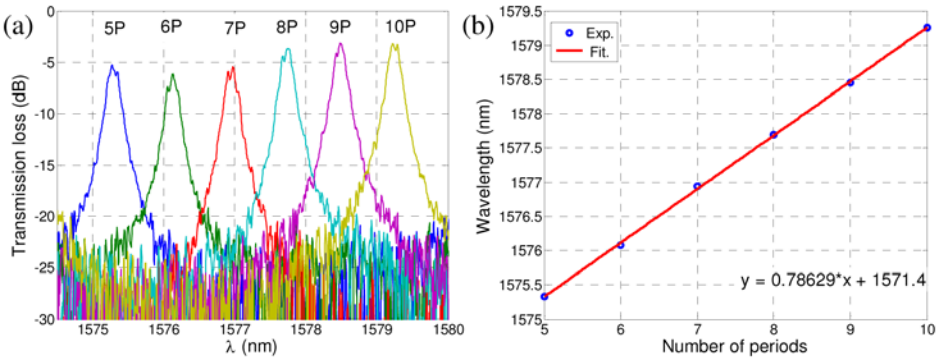

Fig. 8. (a) Measured transmission spectra upon different polymer periods. (b) Linear fitting of resonance wavelengths of the sensing ring.

5. Discussion

We believe that the electrical tracing-assisted microring sensing system offers an alternative to the conventional sensing method. By using the broadband light source (such as super-luminescence diode and LED), power meter and power supplier, we can significantly low down the cost of the sensing system compared to the wavelength-scanning method, which requires high-resolution wavelength tunable lasers. Furthermore, in the wavelength-scanning method, the detection limit is mainly limited by the wavelength resolution of the tunable laser. As it is difficult to obtain extremely high-resolution tunable lasers, the detection limit would be ultimately limited by the instruments. However, in the proposed sensing system, the detection limit is limited by the resolution of the power supplier, which is relatively easy to achieve high-resolution. Besides, the system can be improved by integrate with other components, e.g. the Ge photodetectors to directly read out the powers.

Our proof-of-principle demonstration shows comparable detection limit with the conventional wavelength-scanning method. We believe that the detection limit can be further

#156193 - $15.00 USD Received 10 Oct 2011; revised 9 Nov 2011; accepted 10 Nov 2011; published 6 Feb 2012

improved by microring structure design, such as use of slot-waveguide microring resonators [23], using undercut method to reduce the electrical voltage [24], and the adoption of high-quality power supplier.

6. Conclusion

We proposed a dual-microring resonator-based optical sensing system by using electrical tracing technique. Such system comprises one sensing microring and another tracing microring with electrical tunability. By tracing the resonance shift of the sensing microring via supplying electrical power to the tracing microring, the refractive index change of the sensing microring can be determined by the supplied power. The merit of such sensing scheme is the elimination of the high-resolution wavelength-tunable laser required in the wavelength-scanning method system, which significantly low down the cost. Proof-of-principle demonstration in silicon platform by testing the polyelectrolyte multilayer $(PSS/PAH)_N$ shows the sensing sensitivity of ~4.0 $mW/ng \cdot mm^{-2}$ and the detection limit of ~5.35 pg/mm^2.

Acknowledgments

This work was supported by program for New Century Excellent Talents in University (NCETU), Nature Science Funding of China, NSFC (61177090) and SERC ASTAR.

#156193 - $15.00 USD Received 10 Oct 2011; revised 9 Nov 2011; accepted 10 Nov 2011; published 6 Feb 2012